

Conductive Glassy Nonconjugated Open-Shell Radical Polymer with Organosulfur Backbone for Macroscopic Conductivity

Quyen Vu Thi, Quynh H. Nguyen, Yong-Seok Choi, Seung-Yeol Jeon,* Bryan W. Boudouris,* and Yongho Joo*



Cite This: *JACS Au* 2024, 4, 690–696



Read Online

ACCESS |

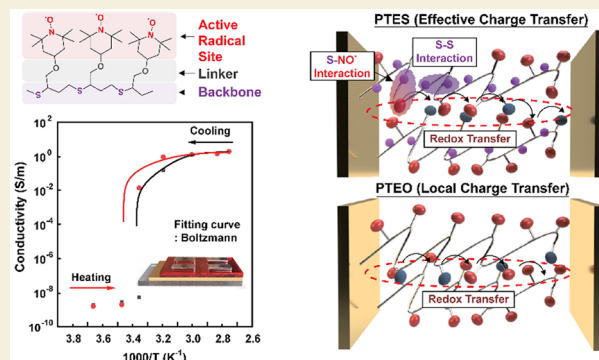
Metrics & More

Article Recommendations

Supporting Information

ABSTRACT: Nonconjugated organic radicals with an open-shell radical active group exhibit unique functionality due to their radical pendant site. Compared with the previously studied doped conjugated polymers, radical polymers reveal superior processability, stability, and optical properties. Despite the success of organic radical polymer conductors based on the TEMPO radicals, it still requires potential design substitutions to meet the fundamental limits of charge transport in the radical polymer. To do so, we demonstrate that the amorphous, nonconjugated radical polymer with backbone–pendant group interaction and low glass transition temperature enables the macromolecules to have rapid charge transport in the solid state, resulting in conductivity higher than 32 S m^{-1} . This charge transport is due to the formation of the local ordered regime with an energetically favored orientation caused by the strong coupling between the backbone and pendant group, which can significantly modulate the polymer packing with active electronic communications. The nonconjugate nature of the radical polymer maintains an optical transparency up to 98% at a $1.5 \mu\text{m}$ thick film. Thus, this effort will be a dramatically advanced model in the organic radical community for the creation of next-generation polymer conductors.

KEYWORDS: radical polymer, conductor, glass transition temperature, optical transparent, sulfur backbone heteroatoms, polymer backbone bonding angle



INTRODUCTION

Air-stable open-shell organic radical polymers are an emerging class of materials for future electronic applications including energy storage devices,^{1–11} transparent displays,^{12–17} memory devices,^{16,18–21} solar cells,²² and spintronics.^{23–25} Compared with the conventional conjugated organic materials that require chemical doping or a high degree of crystallinity for high electrical conductivity, amorphous, undoped, and nonconjugated radical polymers can enable tunable and robust conductivity and optical transparency for myriad applications. In radical polymers, the electronic charge transport occurs through the high-density active radical sites upon reduction–oxidation self-exchange reactions.^{3,4,6} The tunable chemical design of polymeric radicals allows a potentially enormous range of open-shell groups to be combined with varying backbones to tune electronic properties in a powerful manner.²⁶ PTMA was used as the initial organic radical conductor. The champion electronic conductivity ($\sim 20 \text{ S m}^{-1}$) of radical polymers was reported in 2018 with the ether-oxygen-based organic radical polymer within the channel distance of 600 nm or less.^{5,13,27} While this poly(4-glycidioxy-2,2,6,6-tetramethylpiperidine-1-oxyl) (PTEO) exhibits the champion performance, the ultimate performance of radical

polymers still needs to improve.^{3,5,15} To address this point, it is essential to establish the charge transport properties of open-shell chemistries with the understanding of structure–function relationships and design strategies of the alternative chemical structure of radical polymers for the quantification of their potential impact.

RESULTS AND DISCUSSION

In this study, we demonstrate the enhancement of charge transport in radical polymers by surpassing the limitations imposed by channel dimensions. The effective channel distance was upscaled from the microscale to the mesoscale, aligning directly with the charge transport regime of amorphous radical polymers achieved through meticulous molecular design. In particular, polymer poly(TEMPO-substituted ethylene sulfide) (PTES) was synthesized by

Received: November 27, 2023

Revised: January 24, 2024

Accepted: January 25, 2024

Published: February 5, 2024



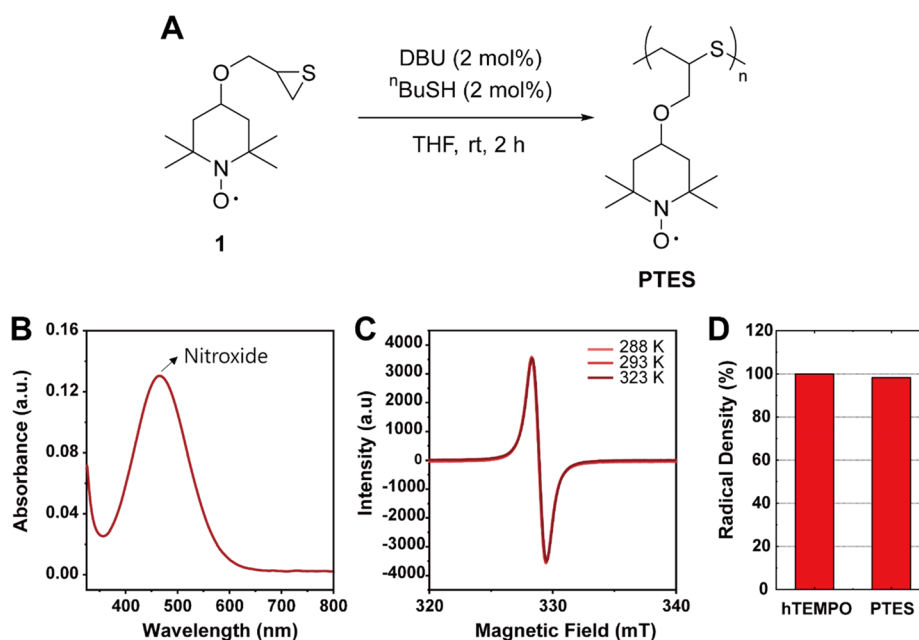


Figure 1. Characterization of the amount of open-shell sites in PTES radical polymers. (A) Anionic ring-opening polymerization for the synthesis of PTES radical polymer. (B) UV-vis spectra of the polymer (in acetone solvent) indicate the presence of a nitroxide pendant group. (C) EPR spectroscopy signal of a radical polymer thin film. (D) Radical density of the PTES polymer used in this work (radical density of above 99%), where the radical density was compared to the hTEMPO small organic radical molecule.

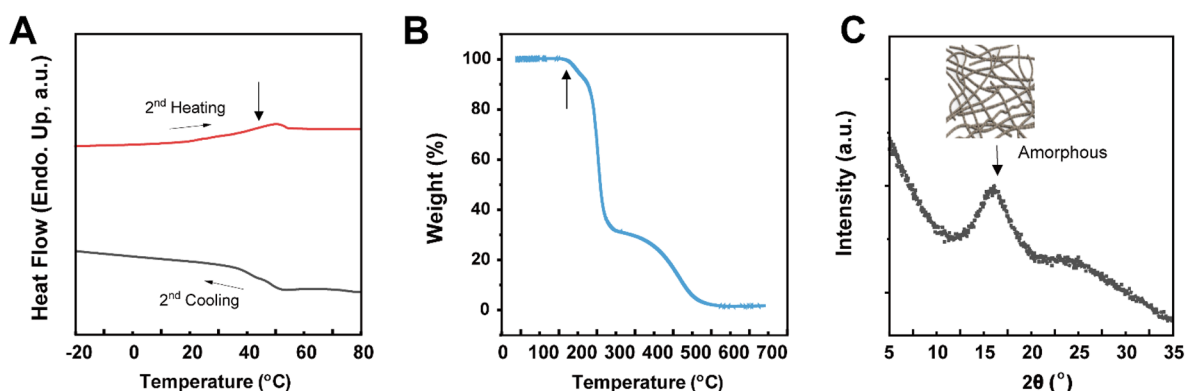


Figure 2. PTES flow, thermal, and percolation properties. (A) DSC curve showing the glass transition temperature of PTES at 50 °C. (B) TGA curve indicating that the degradation temperature of PTES is about 180 °C. (C) XRD, along with the corresponding schematic illustration, reveals the amorphous morphology of the aliphatic polymeric backbone with a bulky nitroxide pendant group.

using a ring-opening anionic polymerization methodology to form a radical polymer with a flexible macromolecular backbone and a relatively low glass transition temperature. The thermal annealing of the PTES radical polymer leads to the formation of percolation domains for macroscopic conductivity with fast charge transfer reactions. The reversible electronic communication of an open-shell active site can be realized by repeating the percolation network above the glass transition temperature (T_g) and insulating the system below T_g in amorphous regimes. This concept is similar to the previous observation for other radical polymers of PTEO; however, the advanced chemical design of radical macromolecule is additionally demonstrated by using the organosulfur backbone in the radical polymer, where the sulfur group could proceed in the self-redox reaction by itself in a rational manner.²⁸ Furthermore, it enhances the overall redox reaction of the radical polymer with the promotion of a nitroxide pendant group that can strongly interact with sulfur (S) of the

backbone, resulting in the enhancement of active units close enough for self-exchange redox reactions of open-shell moieties in the microscale channel device. This not only contrasts strongly with general π -conjugated organic electronics but also represents an advanced design paradigm in the radical polymer electronic society.

The high density of radical active sites is a critical factor in the synthetic design parameters for high-electrical-conductivity radical polymers.^{29,30} It is because the conductivity of radical polymers increased exponentially as the density of the radical region increased.³¹ The well-known strategy to maintain the high density of radical site is to polymerize the monomer that includes an open-shell active site directly for the formation of radical polymer instead of polymerizing a closed-shell monomer and subsequently converting this closed-shell to open-shell species.^{13,16,27,32,33} To do so, the small radical molecule monomer including the nitroxide functionality (thiirane, **1**, Figure 1A) is prepared through the reaction

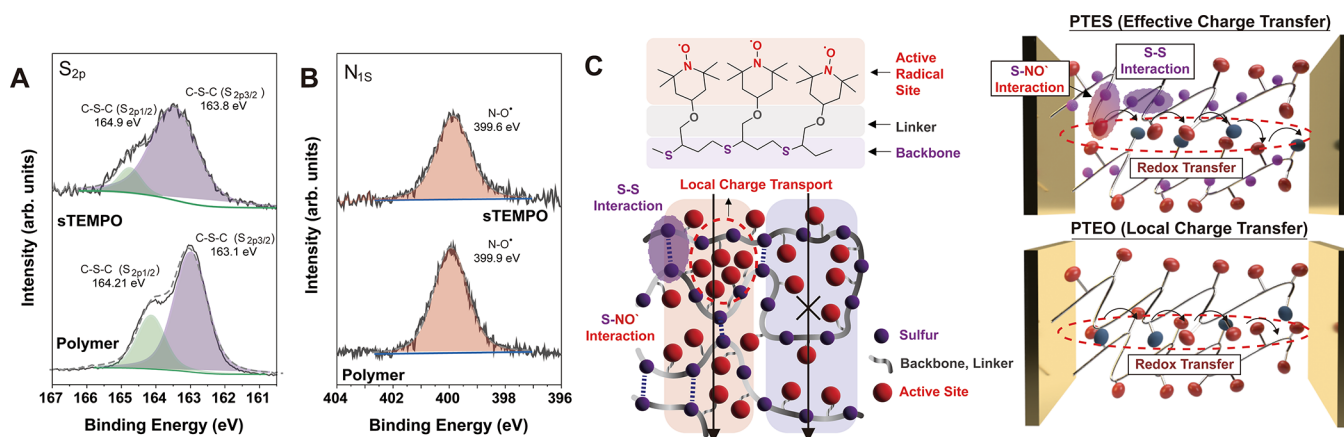


Figure 3. Deconvolution of (A) S_{2p} of monomer and polymer and (B) N_{1s} of monomer and polymer core level XPS spectra for polymer PTES. Typical configuration showing the packing network between active pendant groups and the polymer backbone of PTES to transfer the charges through the local regimes.

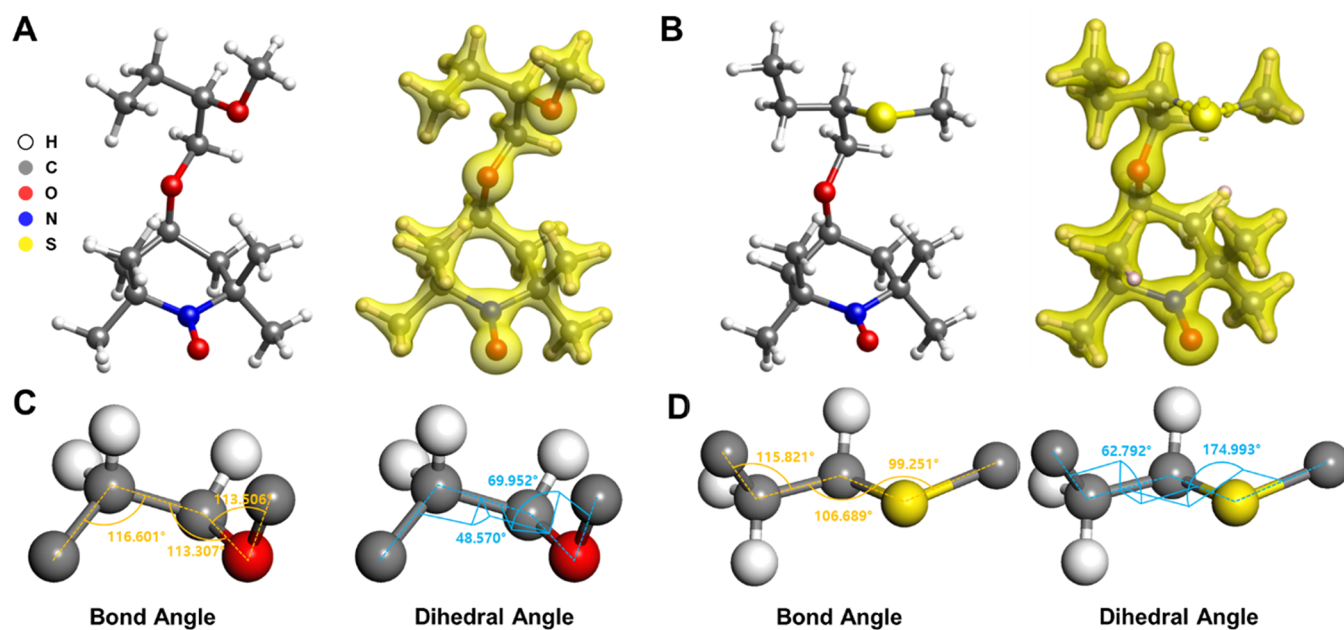


Figure 4. Optimized geometries of repeating units of PTEO and PTES polymers. (A) DFT optimized geometry (left) and charge distribution (right) of the PTEO repeating unit. (B) DFT optimized geometry (left) and charge distribution (right) of the PTES repeating unit. (C) Bond and dihedral angles of the backbone of the repeating unit of PTEO. (D) Bond and dihedral angles of the backbone of the repeating unit of PTES.

between 4-glycidyoxy-2,2,6,6-tetramethylpiperidine-1-oxyl (GTEMPO) and thiourea (see the [Methods](#) section). This small molecular product can be refined to a high level to secure a single pendant radical group per monomer unit. This monomer can participate in an anionic ring-opening polymerization (AROP) in high yield ($\sim 90\%$) with the base ($^t\text{BuSH}$) as the initiator, generating the well-defined PTES radical polymer with a number-average molecular weight of 19.8 kg mol^{-1} . The security of the pendant radical group was indicated by the UV–vis absorption peak (Figure 1B). The PTES maintained a high radical density, above 99%, because the polymerization does not contain the radical intermediate. In addition, with the strong nucleophilicity of the thiolate anion, polymerization of the episulfide monomer was performed at ambient temperature without the need for a strong base ($^t\text{BuOK}$) as an initiator (Figure 1A). A high spin concentration of the radical in the polymer was determined using electron paramagnetic resonance (EPR) spectroscopy (Figure 1C,D).

This result indicated a negligible loss of radical density during the polymerization process and the thermal stability of the radical site in the temperature range $288\text{--}323 \text{ K}$ for solid-state device tests during the heating and cooling of materials.

In addition, another critical design criterion for the high electrical conducting radical polymer is that there should be a large window between the flow transition temperature of the open-shell radical polymer and the degradation temperatures of the pendant group. In this aspect, PTES exhibits a low glass transition temperature of $50 \text{ }^\circ\text{C}$ (Figure 2A), which is far below the degradation temperature of PTES ($180 \text{ }^\circ\text{C}$, Figure 2B).

Due to the high reorganization energies and relatively low electronic coupling to other types of radical moieties, the nitroxide radicals are considered to have some limitation to a certain level of charge transfer with the coupling of the active site in the nonequilibrium amorphous packing structure (Figure 2C).³⁴ In the solid state, the radical site is required

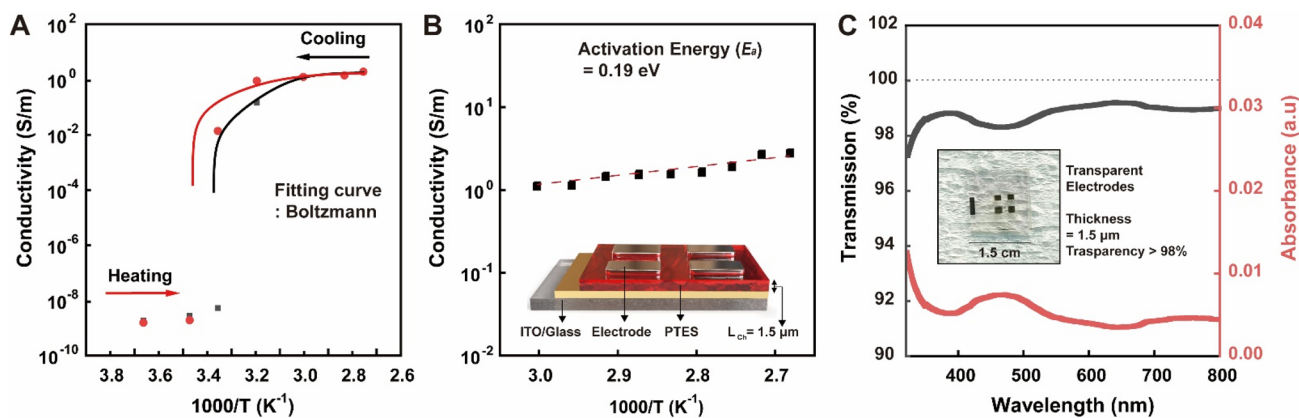


Figure 5. Conducting organic radical and optical properties. (A) Conductivity of PTES at a high-temperature region above T_g . Inset: hysteresis on electrical conductivity versus temperature for PTES at the channel size of $1.5 \mu\text{m}$. (B) Schematic showing the sandwich structure device channel. (C) UV-vis absorption/transmission profile of a $1.5 \mu\text{m}$ thick PTES film on an ITO glass substrate.

to be close enough for rapid redox kinetics. To do so, a molecular design approach to the redox-active radical polymer is required to promote high charge transfer orientation. The PTES material with a low glass transition temperature (T_g) undergoes a phase change from the solid state to molten state to create the percolating nitroxide network for charge transport while keeping it away from the degradation temperature of the radical. This type of design can be tailored with radical polymers, as the macromolecular backbone dominates the mechanical and thermal properties, and pendant chains separated from the backbone dictate the dominant electrochemical properties of the material.²⁷ In Figure 3A, the S_{2p} spectrum of both PTES and the monomer can be analyzed to reveal two predominant peaks at 164.9 and 163.8 eV, corresponding to $S 2p_{1/2}$ and $S 2p_{3/2}$ of the $-C-S-C-$ moiety in the monomer.^{35–37} These peaks exhibit a shift to 164.21 and 163.1 eV in the polymer, attributed to the significant inter- or intramolecular interactions. (Figure 3C) Furthermore, in PTES, the active radical group NO of the monomer, which initially had a binding energy of 399.6 eV, underwent a shift to 399.9 eV (Figure 3B). XPS provides evidence of coupling between the backbone–pendant group ($S-NO$) and the pendant group–pendant group ($NO-NO$) as depicted in the illustration of Figure 3C. Further experimental analysis using FT-IR and UV/vis spectroscopy supports the interaction between sulfur and radical active groups, characterized by the peak shift of the nitroxide group from 460 nm (monomer) to 444 nm (polymer). Instead, no clear peak shift of nitroxide was observed in the FTIR analysis. PTES shows effective charge transfer due to the strong couplings which trigger the favorable orientation of the pendant group with annealing for redox reaction for electronic communication in an amorphous regime compared to the PTEO. The energetically preferred orientation due to the strong coupling between the backbone and the pendant group can potentially be substantially regulated by the details of the polymer packing.³⁸

The origins of PTES's ability to maintain high conductivity on a micrometer (μm) length scale were further explored through density functional theory (DFT) simulations. We performed geometry optimization on repeat units of PTES and identically on repeat units of PTEO as controls (Figure 4). Upon examination of the charge distribution in the optimized structures, it was found that while the oxygen atoms in the

PTEO repeat unit had a relatively greater concentration of electrons, the overall distribution of charges was even throughout the unit (Figure 4A). Compared to the charge distribution observed in PTEO, the distribution near the sulfur atom of PTES's backbone chain exhibited the most significant difference, with almost no charges detected near the sulfur atom and a noticeable concentration of electrons toward the adjacent carbon atoms on both sides (Figure 4B). The electron-donating nature of the sulfur-containing backbone in PTES has the potential to impact intermolecular interactions between polymer chains, which could lead to improved packing and overall material stability. In addition, upon comparison of the bond and dihedral angles of PTES and PTEO backbones (Figures 4C and 4D), it was observed that there was no significant difference in the bond angle. However, in terms of the dihedral angle, the PTEO backbone containing oxygen was curved at around 70° , while the PTES backbone containing sulfur was almost flat at approximately 175° . That is to say, the PTES backbone containing flexible and planar thioethers ($C-S-C$) is believed to provide greater structural diversity by virtue of its ability to adopt various conformations. This is in line with molecular simulation results that optimize polymer structures with geometric variables for torsion angles and tacticity between repeat units based on the DFT optimized structure. Examining the relative conformational energy, defined as the difference between the potential energy of the initial configuration and the optimized configuration, reveals that PTES exhibits more robust conformational flexibility, as it has a lower conformational energy compared to PTEO (Figures S5 and S6). The strong conformational flexibility enables them to possess a wider range of potential percolation pathways for conductivity.

The thermally activated conductivity behavior of PTES was scanned from the low to high charge transport regime versus time during the real transition state of PTES from the glassy state into the molten state. We note that understanding charge transport in radical polymers involves radical-mediated hopping through active pendant groups through the redox self-exchange reaction, forming percolation domains for efficient nanometer- to micrometer-scale charge transport. Influential factors include the molecular structure, polymer morphology, doping, impurities, and temperature. Optimizing these factors is crucial for tailoring the electrical properties. The PTES thin film stayed at its glassy state below T_g before

raising the temperature. When the temperature was greater than T_g , the conductivity of PTES increased by more than 9 orders of magnitude; that is, it went from $\sim 1.8 \times 10^{-9}$ to 1.92 S m^{-1} (Figure 5A). The conductivity was calculated with Ohm's law of $\sigma = L/RA$ (σ is conductivity, R is resistance, L is channel length, and A is channel area) extracted by the slope of the IV curve from DC measurement. The device construction is shown in the inset of Figure 5B with a thickness channel size of $1.5 \mu\text{m}$. Interestingly, the radical polymer exhibited reversible electronic conducting behavior following the heating and cooling process. It demonstrates that charge transport regimes occur through the increased chain dynamics of the radical polymer that has an amorphous morphology, which activates the strong interaction between radical pendant groups to communicate with each other.³⁹ Alternative electrode materials were used to observe the varying conductivity of PTES. The electrical conductivity of PTES was experimentally extracted to be 1.92, 12.1, 26.4, and 32.0 S m^{-1} for electrode materials of platinum (Pt), copper (Cu), silver (Ag), and gold (Au), respectively (Figure S7A) (contact resistance = $0.2 \times 10^4 \Omega$, Figure S8), which exceed the conductivity of radical polymer of PTEO even in the micrometer channel with air stability (Figure S9). To explain this observation, the SOMO of PTES was extrapolated to be 5.09 eV through a cyclic voltammetry plot (Figure S10). In general, besides the molecular structure, band/energy level modulation in the junction of metal/molecules is a critical factor governing the current molecular electronics.^{40,41} As shown in the schematic energy band diagram (Figure S7B), the lowest difference in barrier height between the Au work function and the SOMO energy of the radical polymer is attributed to the favoring of charge transport, resulting in the high collected current for PTES under junction contact.⁴² Such a large electronic conductivity value also provides evidence of the good electron transfer of the PTES radical polymer to the Au electrode.

CONCLUSION

In summary, we have developed the advanced design of a radical polymer of poly(TEMPO-substituted ethylene sulfide) (PTES) working as the transparent conductor sustained over a micrometer (μm) length scale. The complementary backbone design tailored the electrical conductivity values of the nonconjugated open-shell radical polymer above 32 S m^{-1} as optically transparent, charge-neutral conductors. The effective charge transport performance of radical polymers is systematically demonstrated by examining their physical and chemical characteristics. The presence of this regime offers a unique method for controlling the structure of future generations of such macromolecules containing unpaired electrons through molecular engineering.

ASSOCIATED CONTENT

Supporting Information

The Supporting Information is available free of charge at <https://pubs.acs.org/doi/10.1021/jacsau.3c00743>.

Additional experimental details, methods, materials characterizations, detailed data evaluation, and detail spectral assignment reference (PDF)

AUTHOR INFORMATION

Corresponding Authors

Seung-Yeol Jeon – Institute of Advanced Composite Materials, Korea Institute of Science and Technology (KIST), Wanju-gun, Jeonbuk 55324, Republic of Korea; Email: syjeon@kist.re.kr

Bryan W. Boudouris – Charles D. Davidson School of Chemical Engineering, Purdue University, West Lafayette, Indiana 47906, United States; Department of Chemistry, Purdue University, West Lafayette, Indiana 47906, United States; orcid.org/0000-0003-0428-631X; Email: boudouris@purdue.edu

Yongho Joo – Institute of Advanced Composite Materials, Korea Institute of Science and Technology (KIST), Wanju-gun, Jeonbuk 55324, Republic of Korea; Division of Nano and Information Technology, KIST School, Korea University of Science and Technology (UST), Jeonbuk 55324, South Korea; orcid.org/0000-0002-1149-9105; Email: yjoo0727@kist.re.kr

Authors

Quyen Vu Thi – Institute of Advanced Composite Materials, Korea Institute of Science and Technology (KIST), Wanju-gun, Jeonbuk 55324, Republic of Korea; Institute of Sustainability for Chemicals, Energy and Environment (ISCE2), Agency for Science, Technology and Research (A*STAR), Singapore 627833, Republic of Singapore

Quynh H. Nguyen – Institute of Advanced Composite Materials, Korea Institute of Science and Technology (KIST), Wanju-gun, Jeonbuk 55324, Republic of Korea

Yong-Seok Choi – Institute of Advanced Composite Materials, Korea Institute of Science and Technology (KIST), Wanju-gun, Jeonbuk 55324, Republic of Korea

Complete contact information is available at: <https://pubs.acs.org/doi/10.1021/jacsau.3c00743>

Author Contributions

Q.V.T. and Q.H.N. contributed equally to this work.

Notes

The authors declare no competing financial interest.

ACKNOWLEDGMENTS

This work was supported by the Korea Institute of Science and Technology (KIST, Korea) Institutional Program (Project No. 2Z07054, 2E32634). This work was supported by the National Research Foundation of Korea (NRF) grant funded by the Korean government (MSIT) (No. RS-2023-00208313 and 2022K1A3A1A91093969).

REFERENCES

- (1) Tokue, H.; Kakitani, K.; Nishide, H.; Oyaizu, K. Redox mediation through TEMPO-substituted polymer with nanogap electrodes for electrochemical amplification. *Chem. Lett.* **2017**, *46* (5), 647–650.
- (2) Li, F.; Wang, S.; Zhang, Y.; Lutkenhaus, J. L. Electrochemical energy storage in poly(dithieno[3,2-b:2',3'-d]pyrrole) bearing pendant nitroxide radicals. *Chem. Mater.* **2018**, *30* (15), 5169–5174.
- (3) Wang, S.; Easley, A. D.; Lutkenhaus, J. L. 100th Anniversary of Macromolecular Science Viewpoint: Fundamentals for the Future of Macromolecular Nitroxide Radicals. *ACS Macro Lett.* **2020**, *9* (3), 358–370.

- (4) Sato, K.; Ichinoi, R.; Mizukami, R.; Serikawa, T.; Sasaki, Y.; Lutkenhaus, J.; Nishide, H.; Oyaizu, K. Diffusion-cooperative model for charge transport by redox-active nonconjugated polymers. *J. Am. Chem. Soc.* **2018**, *140* (3), 1049–1056.
- (5) Lutkenhaus, J. A radical advance for conducting polymers. *Science* **2018**, *359* (6382), 1334–1335.
- (6) Wang, S.; Li, F.; Easley, A. D.; Lutkenhaus, J. L. Real-time insight into the doping mechanism of redox-active organic radical polymers. *Nat. Mater.* **2019**, *18* (1), 69–75.
- (7) Ma, T.; Easley, A. D.; Thakur, R. M.; Mohanty, K. T.; Wang, C.; Lutkenhaus, J. L. Nonconjugated Redox-Active Polymers: Electron Transfer Mechanisms, Energy Storage, and Chemical Versatility. *Annu. Rev. Chem. Biomol. Eng.* **2023**, *14* (1), 187–216.
- (8) Oyaizu, K.; Ando, Y.; Konishi, H.; Nishide, H. Nernstian adsorbate-like bulk layer of organic radical polymers for high-density charge storage purposes. *J. Am. Chem. Soc.* **2008**, *130* (44), 14459–14461.
- (9) Janoschka, T.; Hager, M. D.; Schubert, U. S. Powering up the Future: Radical Polymers for Battery Applications. *Adv. Mater.* **2012**, *24* (48), 6397–6409.
- (10) Li, C.-H.; Tabor, D. P. Discovery of lead low-potential radical candidates for organic radical polymer batteries with machine-learning-assisted virtual screening. *J. Mater. Chem. A* **2022**, *10* (15), 8273–8282.
- (11) Ji, L.; Shi, J.; Wei, J.; Yu, T.; Huang, W. Air-Stable Organic Radicals: New-Generation Materials for Flexible Electronics? *Adv. Mater.* **2020**, *32* (32), 1908015.
- (12) He, J.; Mukherjee, S.; Zhu, X.; You, L.; Boudouris, B. W.; Mei, J. Highly transparent crosslinkable radical copolymer thin film as the ion storage layer in organic electrochromic devices. *ACS Appl. Mater. Interfaces* **2018**, *10* (22), 18956–18963.
- (13) Akkiraju, S.; Vergados, J.; Hoagland, L.; Lu, Z.; Anandan, V.; Boudouris, B. W. Design of Mixed Electron- and Ion-Conducting Radical Polymer-Based Blends. *Macromolecules* **2021**, *54* (11), 5178–5186.
- (14) Yu, I.; Jo, Y.; Ko, J.; Kim, D.-Y.; Sohn, D.; Joo, Y. Making Nonconjugated Small-Molecule Organic Radicals Conduct. *Nano Lett.* **2020**, *20* (7), 5376–5382.
- (15) Yu, I.; Jeon, D.; Boudouris, B.; Joo, Y. Mixed Ionic and Electronic Conduction in Radical Polymers. *Macromolecules* **2020**, *53* (11), 4435–4441.
- (16) Oyaizu, K.; Nishide, H. Radical polymers for organic electronic devices: a radical departure from conjugated polymers? *Adv. Mater.* **2009**, *21* (22), 2339–2344.
- (17) Jo, Y.; Yu, I.; Ko, J.; Kwon, J. E.; Joo, Y. Sequential Codoping Making Nonconjugated Organic Radicals Conduct Ionically Electronically. *Small Sci.* **2022**, *2* (1), 2100081.
- (18) Yonekuta, Y.; Susuki, K.; Oyaizu, K.; Honda, K.; Nishide, H. Battery-inspired, nonvolatile, and rewritable memory architecture: a radical polymer-based organic device. *J. Am. Chem. Soc.* **2007**, *129* (46), 14128–14129.
- (19) Singh, D.; Magnan, F.; Gilroy, J. B.; Fanchini, G. Electro-tunable Radical Polymers for Thin-Film Electronic Device Applications. *ECS Trans.* **2022**, *108* (1), 17.
- (20) Suga, T.; Sakata, M.; Aoki, K.; Nishide, H. Synthesis of pendant radical-and ion-containing block copolymers via ring-opening metathesis polymerization for organic resistive memory. *ACS Macro Lett.* **2014**, *3* (8), 703–707.
- (21) Lee, J.; Lee, E.; Kim, S.; Bang, G. S.; Shultz, D. A.; Schmidt, R. D.; Forbes, M. D. E.; Lee, H. Nitronyl Nitroxide Radicals as Organic Memory Elements with Both *n*- and *p*-Type Properties. *Angew. Chem., Int. Ed.* **2011**, *50* (19), 4414–4418.
- (22) Chen, Z. X.; Li, Y.; Huang, F. Persistent and Stable Organic Radicals: Design, Synthesis, and Applications. *Chem.* **2021**, *7* (2), 288–332.
- (23) Tan, Y.; Hsu, S.-N.; Tahir, H.; Dou, L.; Savoie, B. M.; Boudouris, B. W. Electronic and Spintronic Open-Shell Macromolecules, Quo Vadis? *J. Am. Chem. Soc.* **2022**, *144* (2), 626–647.
- (24) Mukherjee, S.; Boudouris, B. W. *Organic Radical Polymers: New Advances in Organic Electronics*; Springer: 2017.
- (25) Fedin, M.; Ovcharenko, V.; Sagdeev, R.; Reijerse, E.; Lubitz, W.; Bagryanskaya, E. Light-Induced Excited Spin State Trapping in an Exchange-Coupled Nitroxide-Copper(II)-Nitroxide Cluster. *Angew. Chem., Int. Ed.* **2008**, *47* (36), 6897–6899.
- (26) Zhang, K.; Monteiro, M. J.; Jia, Z. Stable organic radical polymers: synthesis and applications. *Polym. Chem.* **2016**, *7* (36), 5589–5614.
- (27) Joo, Y.; Agarkar, V.; Sung, S. H.; Savoie, B. M.; Boudouris, B. W. A nonconjugated radical polymer glass with high electrical conductivity. *Science* **2018**, *359* (6382), 1391–1395.
- (28) Xu, D.; Liang, M.; Qi, S.; Sun, W.; Lv, L.-P.; Du, F.-H.; Wang, B.; Chen, S.; Wang, Y.; Yu, Y. The Progress and Prospect of Tunable Organic Molecules for Organic Lithium-Ion Batteries. *ACS Nano* **2021**, *15* (1), 47–80.
- (29) Hay, M. E.; Hui Wong, S.; Mukherjee, S.; Boudouris, B. W. Controlling open-shell loading in norbornene-based radical polymers modulates the solid-state charge transport exponentially. *J. Polym. Sci., Part B: Polym. Phys.* **2017**, *55* (20), 1516–1525.
- (30) Baradwaj, A. G.; Wong, S. H.; Laster, J. S.; Wingate, A. J.; Hay, M. E.; Boudouris, B. W. Impact of the addition of redox-active salts on the charge transport ability of radical polymer thin films. *Macromolecules* **2016**, *49* (13), 4784–4791.
- (31) Hay, M. E.; Hui Wong, S.; Mukherjee, S.; Boudouris, B. W. Controlling open-shell loading in norbornene-based radical polymers modulates the solid-state charge transport exponentially. *J. Polym. Sci., Part B: Polym. Phys.* **2017**, *55* (20), 1516–1525.
- (32) Rostro, L.; Baradwaj, A. G.; Boudouris, B. W. Controlled radical polymerization and quantification of solid state electrical conductivities of macromolecules bearing pendant stable radical groups. *ACS Appl. Mater. Interfaces* **2013**, *5* (20), 9896–9901.
- (33) Xie, Y.; Zhang, K.; Yamauchi, Y.; Oyaizu, K.; Jia, Z. Nitroxide radical polymers for emerging plastic energy storage and organic electronics: fundamentals, materials, and applications. *Mater. Horiz.* **2021**, *8* (3), 803–829.
- (34) Tan, Y.; Casetti, N. C.; Boudouris, B. W.; Savoie, B. M. Molecular Design Features for Charge Transport in Nonconjugated Radical Polymers. *J. Am. Chem. Soc.* **2021**, *143* (31), 11994–12002.
- (35) Buckel, F.; Effenberger, F.; Yan, C.; Götzhäuser, A.; Grunze, M. Influence of Aromatic Groups Incorporated in Long-Chain Alkanethiol Self-Assembled Monolayers on Gold. *Adv. Mater.* **2000**, *12* (12), 901–905.
- (36) Qie, L.; Chen, W.; Xiong, X.; Hu, C.; Zou, F.; Hu, P.; Huang, Y. Sulfur-Doped Carbon with Enlarged Interlayer Distance as a High-Performance Anode Material for Sodium-Ion Batteries. *Adv. Sci.* **2015**, *2* (12), 1500195.
- (37) Rostro, L.; Wong, S. H.; Boudouris, B. W. Solid state electrical conductivity of radical polymers as a function of pendant group oxidation state. *Macromolecules* **2014**, *47* (11), 3713–3719.
- (38) Caneschi, A.; Ferraro, F.; Gatteschi, D.; Le Tirzini, A.; Novak, M. A.; Rentschler, E.; Sessoli, R. Ferromagnetic order in the sulfur-containing nitronyl nitroxide radical, 2-(4-thiomethyl)phenyl-4,4,5,5-tetramethylimidazole-1-oxyl-3-oxide, NIT(SMe)Ph. *Adv. Mater.* **1995**, *7* (5), 476–478.
- (39) Kemper, T. W.; Gennett, T.; Larsen, R. E. Molecular dynamics simulation study of solvent and state of charge effects on solid-phase structure and counterion binding in a nitroxide radical containing polymer energy storage material. *J. Phys. Chem. C* **2016**, *120* (45), 25639–25646.
- (40) Souto, M.; Yuan, L.; Morales, D. C.; Jiang, L.; Ratera, I.; Nijhuis, C. A.; Veciana, J. Tuning the rectification ratio by changing the electronic nature (open-shell and closed-shell) in donor-acceptor self-assembled monolayers. *J. Am. Chem. Soc.* **2017**, *139* (12), 4262–4265.
- (41) De Sousa, J. A.; Pfaltner, R.; Gutiérrez, D.; Jutglar, K.; Bromley, S. T.; Veciana, J.; Rovira, C.; Mas-Torrent, M.; Fabre, B.; Crivillers, N. Stable Organic Radical for Enhancing Metal-Monolayer-Semiconduc-

tor Junction Performance. *ACS Appl. Mater. Interfaces* **2023**, *15* (3), 4635–4642.

(42) Xie, Y.; Wang, C.-Y.; Chen, N.; Cao, Z.; Wu, G.; Yin, B.; Li, Y. Supramolecular Memristor Based on Bistable [2]Catenanes: Toward High-Density and Non-Volatile Memory Devices. *Angew. Chem., Int. Ed.* **2023**, *62* (42), No. e202309605.